AIAA–2002–0557

A Quantitative Comparison of Leading-Edge Vortices in Incompressible and Supersonic Flows

F.Y. Wang
NASA Glenn Research Center
Cleveland, OH

I.M. Milanovic
University of Hartford
West Hartford, CT

K.B.M.Q. Zaman
NASA Glenn Research Center
Cleveland, OH

40th AIAA Aerospace Sciences Meeting & Exhibit
January 14–17, 2002 / Reno, NV

AIAA-2002-0557

A QUANTITATIVE COMPARISON OF LEADING-EDGE VORTICES IN INCOMPRESSIBLE AND SUPERSONIC FLOWS

F. Y. Wang*, I. M. Milanovic† and K. B. M. Q. Zaman‡

Abstract

When requiring quantitative data on delta-wing vortices for design purposes, low-speed results have often been extrapolated to configurations intended for supersonic operation. This practice stems from a lack of database owing to difficulties that plague measurement techniques in high-speed flows. In the present paper an attempt is made to examine this practice by comparing quantitative data on the near-wake properties of such vortices in incompressible and supersonic flows. The incompressible flow data are obtained in experiments conducted in a low-speed wind tunnel. Detailed flow-field properties, including vorticity and turbulence characteristics, obtained by hot-wire and pressure probe surveys are documented. These data are compared, wherever possible, with available data from a past work for a Mach 2.49 flow for the same wing geometry and angles-of-attack. The results indicate that quantitative similarities exist in the distributions of total pressure and swirl velocity. However, the streamwise velocity of the core exhibits different trends. The axial flow characteristics of the vortices in the two regimes are examined, and a candidate theory is discussed.

*NRC Fellow, NASA John Glenn Research Center at Lewis Field; Currently Aerospace Engineer at John A. Volpe National Transportation Systems Center, Cambridge, MA, Senior Member AIAA

†Assistant Professor, University of Hartford CT, Member AIAA

‡Arospace Engineer, NASA John Glenn Research Center at Lewis Field, Cleveland OH, Associate Fellow AIAA

1. Introduction

After more than five decades of research, investigations of delta-wing vortices continue to be of both practical and academic importance. However, the available database allowing a quantitative comparison of these vortices between incompressible and supersonic regimes is still very limited. In order to delineate the motivation of the present study, a summary of the current understanding of incompressible and supersonic delta-wing vortices, and hypotheses on how they may compare, are first provided.

For a sharp-edged planform in a low-speed stream, the overall vorticity dynamics is reasonably understood based on visualization as well as quantitative experiments. Flow from windward (pressure) side spilling over the leeward (suction) side separates along the leading-edges. The resulting shear-layers then roll into a pair of large counter-rotating swirls above the delta-wing.

These are commonly referred to as either "primary" or "leading-edge" vortices. The primary vortex pair often would induce a smaller pair of secondary vortices of opposite sign. Sometimes even a pair of tertiary vortex, induced by the secondary vortex pair, can be observed. However, with increasing distance from the planform, the latter vortices decay quickly. Consequently, within a short distance, the leading-edge vortex pair remains as the salient feature of the wake. The process usually completes within just a couple of chords from the planform.[1-4]

In the supersonic flow regime, quantitative investigation has been very rare in comparison to its low-speed counterpart.[5,6] This is due mainly to experimental difficulties encountered in high-speed flows. However in visualization studies, it has been noted that when the leading-edge is swept within the Mach cone generated by the wing apex (i.e., subsonic leading-edge[7]) and when crossflow shock waves do not apparently interact with the vortices, the overall leeward flow topology is relatively insensitive to Mach and Reynolds numbers.[7-14] As for the vortex flow

downstream of the planform at supersonic freestream Mach numbers, they have likewise been envisioned[1,15-18] and shown to exhibit topological similarities[19] with their low-speed counterparts under the condition of subsonic leading-edge. These findings provided a justification for designers and researchers to extrapolate low-speed results to configurations intended for supersonic operations.[8-10] As for measurements in supersonic wake, data can be found in previously classified literature, such as in Refs. 15-18. However, the emphasis of these measurements was not to provide detailed characteristics of the flow field, but to evaluate theoretical models on downwash prediction in the wake at generously spaced intervals. Although these data yielded useful gross information, quantitative data on the supersonic leading-edge vortex remain rare. The lack of basic information such as vortex trajectory downstream of a delta-wing was noted, for example, during interpretation of supersonic vortex mixing data using a delta-wing in the study of Povinelli et. al.[20]

Although evidence exists to support that vortices in the two flow regimes can be qualitatively similar, Green[14] conjectures that quantitative details of the vortices in the two flow regimes are surely different, as are the associated aerodynamic effects. Dissimilarities have been noted in many studies. For example, the onset of vortex asymmetry and vortex breakdown are found to occur at much lower angles-of-attack in supersonic flow compared to their low-speed counterpart.[12,14,21,22] An obvious dissimilarity stems from compressibility effects. Crossflow shock waves can emerge to interact with the primary vortices in the supersonic freestream case. Significant density gradient variation exists as indicated by shadowgraph flow visualization. Thus, it is possible that baroclinic torque could be an additional source of vorticity in the compressible flow regime. Differences are also inferred from leeward surface pressure measurements. For a fixed angle-of-attack, the magnitude of the primary suction peak on the leeward side has been shown to reduce with increasing freestream Mach number.[23,24] This could mean a corresponding decrease in vortex strength. The shape of the primary "vortex core", as visualized by vapor screen technique, has been found to become more flattened with increasing Mach number.[7,25,26] Downstream of the planform, vapor-screen visualization suggests that the primary vortex can experience substantial stretch vertically, and that secondary vortices persist further downstream at higher Mach number.[19]

There are certain physical differences in the basic states between the two flow regimes that could impact the structure of the vortices in the wake. In the low-speed case, Kutta-condition dictates that the leeward flow decelerate after the initial acceleration as the trailing-edge is approached. Thus, the leading-edge vortices themselves are subjected first to a favorable, followed by an adverse pressure gradient over the leeward suction surface. In the supersonic case on the other hand, the flow on the leeward surface would be continually in expansion and then abruptly decelerated by a shock wave from the trailing-edge downstream.

In light of the preceding discussion, it is apparent that there are some conflicting views on how vortical structures in the two flow regimes may differ. The literature lacks a direct quantitative comparison needed for validating theoretical and computational studies. Such an effort constitutes the first objective of the present paper. During the course of the literature survey, it was also apparent that full details of the vortical structure even in a low-speed wake were very much lacking.[2,3,12,14] Such a detailed documentation of the vortex-wake at low-speed, particularly for the turbulence and vorticity characteristics, forms the second objective of the paper.

2. Experimental Setup

Both the supersonic and incompressible experiments were performed with a delta-wing of common geometric proportion, but of two different sizes. Each delta-wing (also referred to as "planform") had 75° sweepback, thus, the apex angle at the leading-edge was 30°. Each was of flat-top shape, having four percent thickness-to-root chord ratio and a chamfer of 30° along all edges. A streamlined strut, attached to the windward side, supported each wing. The Reynolds numbers based on the root chord in the high and low speed experiments were 6.5×10^6 and 1.0×10^5, respectively.

The supersonic experiments were conducted in the Mach 2.49 blowdown facility at the Polytechnic University in Farmingdale, New York; the results were summarized in Refs. 28,29. Measurements were carried out with a five-hole miniature probe, whose mechanical and calibration details were given in Ref. 30. Additional information on the experimental setup, facility and instrumentation were described in Ref. 28. The leading-edge vortex surveys were made at two angles-of-attack (7° and 12°) and at two locations, at the trailing-edge and at half-chord downstream from the trailing-edge. For each combination of survey location and angle-of-attack, two mutually perpendicular traverses though the vortex core were made.

The low-speed experiments were carried out in an open circuit tunnel at NASA Glenn Research Center. The operating condition was essentially incompressible, at a Mach number of 0.02. Two adjacent crossed hot-wires of different orientations were utilized to obtain three components of velocity and turbulence intensity. The hot-wires were traversed under automated computer control for conducting the flow field surveys. Additional information can be found in Ref. 31. An approximately 0.8mm I.D. thin-walled Pitot probe, connected to a 0.1 inch-of-water (24.91 Pa) range pressure transducer, was used to acquire the total pressure data in separate runs. As with the supersonic experiment, the planform was set at 7° and 12° angles-of-attack. Transverse and spanwise surveys through the vortex centers were performed at the trailing-edge and at half-chord downstream from the trailing-edge. In addition, detailed cross-sectional mappings of velocity and total pressure were performed at six different streamwise locations. In both supersonic and low-speed experiments, surveys were carried out on the portside of the planform.

For each angle-of-attack, the coordinate origin is located at the portside apex of the trailing-edge. "Streamwise" coordinate is along the direction of the freestream. "Spanwise" coordinate is in the horizontal direction parallel to the trailing-edge, the other cross-stream coordinate is referred to as "transverse". Although streamwise measurement locations are referred to in terms of the chord of the delta-wing, in the figures all distances are nondimensionalized by half-span of the trailing-edge.

3. Results and Discussions

3.1 Comparison of high and low speed surveys

Results from the two flow regimes are compared, at the trailing-edge in Figs. 1-6 and at half-chord downstream from the trailing-edge in Figs. 7-12. In order to permit the comparison with incompressible flow characteristics, Mach number data from the supersonic experiments were converted to velocity by assuming the stagnation temperature to be a constant. Also, since both sets of experiments employed probes traversing in planes normal to the freestream direction, unless the vortex axis is aligned with the probe axis, the swirl component of the vortex is not truly measured. The term vortex "swirl" velocity is nevertheless used to denote cross-stream velocity components. Similarly, the term "axial" velocity is used to denote streamwise velocity. Velocities and total pressures have been normalized with their respective freestream values, and, as stated earlier, distances are made non-dimensional with respect to the semispan of trailing-edge.

Trailing-edge

The comparison at the trailing-edge station is presented in Figs. 1-6. Profiles in the transverse direction are shown in Figs. 1-3 and those in the spanwise direction are shown in Figs. 4-6. It is noted that the magnitude and spatial extent of total pressure deficits increase with increasing angle-of-attack (Fig. 1). Using minimum Pitot pressure as the indicator, the vortex core center at the $\alpha=7^\circ$ in the Mach 2.49 study[28] was reported, in normalized coordinates, at 0.39 and 0.13 in the spanwise and transverse directions, respectively (see, Figs. 4(a) and 1(a)). At $\alpha=12^\circ$ the core center at the high Mach number was found at (0.54, 0.21). For the low-speed experiments, with a similar criterion, the core centers are found to be at (0.34, 0.15) and (0.41, 0.24), for the 7° and 12° cases, respectively. Both high- and low-speed results show the vortex moving inboard and upward relative to the model surface, as the angle-of-attack is increased. However, the cores in the Mach 2.49 case are slightly more toward the centerline of the wing and closer to the surface compared to the low-speed counterpart.

For the vortex core dimension, a criterion based on the locations of swirl velocity peaks and maximum pressure gradient was used in Ref. 28. According to that criterion, at the Mach 2.49 case at 7°, the core is measured to be 0.29 and 0.14 semispans in the spanwise and transverse directions, respectively. The corresponding dimensions for the Mach 2.49, 12° case are 0.42 and 0.26 semispans. Using the same criterion, the low-speed core dimensions are found to be 0.18 and 0.14 for the 7° case, and 0.12 and 0.19 for the 12° case. The measurements therefore concur with the visualization results that the core shape in the high-speed case is more elongated in the spanwise direction[7,25,26]. This flattening of the core at high-speed is conceivably caused by the expanding flow from the leading-edge that situates above the vortex[7].

The spanwise profiles of total pressure (Fig. 4) also reveal the presence of secondary vortices, as indicated by smaller secondary dips[28,29]. They are to the left of the primary vortices in both sets of experiments. The secondary vortices, found in normalized spanwise range of 0.1-0.25, are characterized by opposite gradients in the transverse velocity (see Fig. 5). It will be shown later for the low-speed case that the swirl is of opposite sense at these locations compared to that of the primary vortex.

Thus the flow fields at the two regimes so far are found to be similar in many details. However, for the

streamwise velocity distributions several differences are observed. In the supersonic case, increasing the angle-of-attack results in a greater deficit of the velocity in the core where the magnitude of the velocity is below that of the freestream. This trend is especially apparent in the transverse traverse results of Fig. 3a. At low-speed, shown in Fig. 3b, the trend is reversed. An increase in angle-of-attack results in the axial velocity in the core to increase, and velocity outside of the core likewise increasingly exceeds that of the freestream value. The streamwise velocity characteristics have important consequence on vortex breakdown in both supersonic and incompressible freestreams[32-35]. A vortex with its core axial velocity being less than that of freestream is more susceptible to breakdown, as the required deceleration in the axial flow to reach a free stagnation point is less than that for either a uniform or an overshoot/jet-like profile. The axial flow characteristics of the vortex core are discussed further in a later session.

Half-chord from trailing-edge

Data at half-chord are compared for the two flow regimes in Figs. 7-12, in a similar manner as done in Figs. 1-6. At Mach 2.49, core centers for the $\alpha=7^\circ$ and 12° cases are located at (0.37, 0.08) and (0.48, 0.11) in their respective normalized coordinates. At Mach 0.02, core center locations are found at (0.29, 0.17) in the $\alpha=7^\circ$ case, and at (0.34,0.19) at $\alpha=12^\circ$. Therefore at each angle-of-attack, both flow regimes showed the cores to have moved slightly outboard while turning toward the freestream direction. The core dimensions are found as follows. At Mach 2.49 and $\alpha=7^\circ$ the core size is 0.22 and 0.18 in the spanwise and transverse directions. At $\alpha=12^\circ$ the corresponding sizes are 0.22 and 0.32. The low-speed core dimensions are found to be 0.22 and 0.23 for the 7° case, and 0.22 and 0.20 for the 12° case. While the cores in the low-speed case are approximately round, the data for the $\alpha=12^\circ$ case at Mach 2.49 suggest that the core is stretched significantly in the transverse direction. The same feature is also noted in Ref. 19, in which vapor-screen visualization of the near-wake flow of a 73° sweptback wing at $\alpha=10^\circ$ in a Mach 2 freestream is presented.

In both flow regimes, the viscous wake of the trailing-edge is evident in the total pressure profiles (around the transverse location of –0.2 in Fig. 7, right below the vortex cores). Nevertheless, "swirl" patterns are still quite discernable, as seen in Fig. 8. The results from the spanwise traverses at high-speed also suggest the presence of a secondary vortex. This is indicated by the total pressure deficit (Fig. 10a) and the swirl velocity profiles (Fig. 11a), in the spanwise range of 0.0-0.1. At low-speed, although the total pressure profiles in regions left of the primary vortex exhibit a deficit, the secondary vortex is not detected in the swirl velocity profiles of Fig. 11b. The low total pressure around the aforementioned spanwise range is caused by the shear-layer from the leading-edge; this becomes clearer with the detailed mappings shown later. It then appears that the secondary vortex generated in the supersonic case is either stronger initially, or has less dissipative characteristics, such that it persists further downstream compared to its low-speed counterpart.

The axial velocity characters at half-chord, particularly in the high-speed case, are rather complex. This is thought to be in part due to the vortex being immersed in the near-wake and entrainment of the separated flow from the trailing-edge. In the Mach 2.49 experiment, shadowgraph visualization showed that the trailing vortices had gone through the shock and expansion waves generated by the trailing-edge prior to reaching the half-chord survey location. At high angle-of-attack, the low-speed vortices are again found to be propelled towards higher velocity region. At low-speed, unlike the results at the trailing-edge, the minimum velocities in the core are found to be lower than that of the freestream. The results here have shown that vortices in the two flow regimes can have similar characteristics of the core with comparable swirl profiles, however, the corresponding axial velocity distributions can be quite different. Their causes and implications are further explored in the following section.

Axial flow in the vortex core

Concurring with experience reported in the literature, the present experiments show that vortices do not necessarily convect at uniform speed. When the core flow velocity is higher than the freestream velocity, a vortex is described as having a jet-like profile. Similarly, a wake-like profile refers to a vortex having the core velocity lower than that of the freestream. The mechanisms affecting the axial flow character of an incompressible trailing vortex was first addressed by Batchelor.[36] According to his analysis, the axial velocity at a given radial location is determined by evaluating the following equation from a point within the vortex to the outer freestream flow:

$$u^2 = u_\infty^2 + \int_r^\infty \frac{1}{r^2}\frac{\partial C^2}{\partial r}\,dr - 2\Delta H \qquad (1)$$

where, $C \equiv rw$, is the circulation parameter with w being the swirl velocity, and ΔH being the integrated total pressure loss. Note that for a typical linear swirl profile in the core, the contribution of the integral term will be positive, thereby promoting the axial flow to be jet-like. On the other hand, the total pressure loss will retard the axial flow into a wake-like profile. It should

be noted that Eq. (1) was derived during an investigation of wing-tip vortices, but the basic integral formulation is applicable and independent of the specific vortex generator.

Wang and Sforza[37] later extended the formulation of Batchelor[36] to compressible flow by assuming a polytropic relation in the core. A similar expression was obtained:

$$u^2 = u_\infty^2 + \left[7\left(\frac{n-1}{n}\right) - 2\right] \int_r^\infty \frac{C^2}{r^3} dr + \int_r^\infty \frac{1}{r^2} \frac{\partial C^2}{\partial r} dr - 2\Delta H \qquad (2)$$

where n is the polytropic exponent, and ΔH is now the stagnation enthalpy loss. Note that Eq. (2) differs from Eq. (1) in an extra term involving the circulation parameter and the representation of the viscous loss. It then follows that for a viscous core, $1 < n < 1.4$ and $C = rw = Ar^2$ where A is a constant, the first integral of the circulation parameter will be negative. However, the net contribution from the two terms involving C is positive. Thus, the same mechanisms affecting the axial flow in incompressible fluid are found to apply in compressible regime.

In both flow regimes, vortex circulation is shown to promote a jet-like profile, whereas viscous loss from the lifting surface entrained into the core drives a wake-like profile. Hence, the axial flow profile is ultimately dictated by the interaction of the vortex circulation and viscous loss stemming from the boundary layer flow. It is thus possible to have both velocity overshoot and deficit in the axial flow profile existing in the same cross section at different radii. Although instrumental in delineating the physical mechanisms, due to difficulty in quantifying the viscous loss from a three-dimensional separated flow, Eqs. (1) and (2) do not readily lead to quantitative predictions. Nevertheless, further qualitative assessment of the axial flow behavior on the basis of these integral formulations can be made.

First, an examination of Eqs. (1) and (2) leads to the observation that for identical circulation produced in high- and low-speed streams, the compressible counterpart would have less capacity to promote a jet-like axial flow due to the first term involving C. Thus, for a theoretical situation where viscous loss in the two flow regimes is the same, the extent of the axial flow overshoot, if exists, would be less in the compressible flow case. It is also pertinent to consider the ideal amount of circulation a planform could impart into its wake. If it is assumed that the entire lift of the planform manifests itself in the vortex-wake such that the Kutta-Joukowski relationship were applicable, then the non-dimensional vortex circulation becomes half of the lift coefficient. Hence, the lift coefficient is an approximate indicator of the strength of the vortex produced. The supersonic experimental data provided in Ref. 27 showed that lift coefficient, for a 76° sweepback subsonic leading-edge delta-wing, varies inversely with freestream Mach number at a given angle-of-attack. Hence, the circulation produced can be assumed to reduce with increasing Mach number. Compounded by the first term in the compressible formulation of the axial flow equation, a vortex in compressible flow will more likely be dominated by the viscous loss term in Eq. (2) to result a wake-like profile. This is in agreement with the Mach 2.49 data at both survey locations.

At low-speed, it is conjectured that the gain in circulation by the increase in angle-of-attack is able to offset the corresponding viscous loss. Thus, the overall core axial velocity overshoot is progressively greater as the planform incidence increases, with the exception of a narrow region near the core center where the viscous loss from the vortex generation process is entrained and concentrated. Although there exists a locally "wake-like" velocity profile (Fig. 3b), it is noted that the magnitude of the deficit is nevertheless slightly over the freestream value. It should be mentioned here that the jet-like core velocities found at the trailing-edge at low-speed are in good agreement with past measurements for similar delta-wing configuration.[39] With increasing downstream distance, additional dissipative effect from the ingestion of the turbulent wake from the trailing-edge continue to compete through the ΔH term of Eq. (1). Thus, a wake-like profile may eventually evolve, as seen in the half-chord downstream.

3.2 Detailed mapping at low-speed

Detailed measurements were made at low-speed for the two angles-of-attack at six locations starting from the trailing-edge to 0.65 root chord downstream. For brevity, results are shown only for the 12° case, in Figs. 13-16. The downstream evolution of the vortex properties is summarized in Fig. 17.

Results of Figs. 1b, 4b, 7b and 10b revealed that there existed substantial total pressure deficit in the cores of leading-edge vortices. This attribute is confirmed on a global perspective through the total pressure maps shown in Fig. 13. The contours associated with the vortex cores are quite distinguishable. Significantly lower pressures characterize the cores. Another

structure of low total pressure is observed underneath the leading-edge vortex, which is believed to be a combination of the secondary vortex and the shear-layer from the trailing-edge of the planform. For the first two stations of the survey, the trailing-edge shear-layer and secondary vortex also had very pronounced total pressure deficit. This disappears quickly with increasing downstream distance while merging with the primary vortex. Near the trailing-edge, the measured total pressure (normalized by that of freestream) in the leading-edge vortex core had a value of 0.09. This recovered to 0.11 at the last survey location.

In Fig. 14, the contours of turbulence intensity are shown. The cross-stream velocity vector fields are superimposed in this and the rest of the plots in Figs. 14-16. Peak turbulence intensity in the core is found to be 11 percent at the trailing-edge plane. The shear-layers from the trailing-edge and leading-edge separation are also discernible. These manifest themselves as a highly turbulent sheet of fluid wrapping around the primary vortex. Consistent with the evolution depicted from total pressure contours of Fig. 13, the shear-layers from the trailing-edge is seen to be ingested by the primary vortex farther downstream. The turbulence intensity at the end of the survey limit is found to be 0.16, representing a significant increase of 45 percent. The high turbulence intensity found in the vortex core is often thought of as an artifact of meandering. The hot-wire measurements suggest that entrainment of the highly turbulent fluid surrounding the vortex would have also contributed to the final high turbulence intensity in the core.

In Fig. 15, streamwise vorticity contours are shown. The primary as well as secondary vortices are clearly identified. The ingestion of the surrounding turbulent fluid into the core and turbulent diffusion are believed to be responsible for the rapid decrease in the streamwise vorticity with increasing distance from the trailing-edge. The senses of the swirl at the primary and secondary vortices are clearly seen from the vector fields. The normalized total velocity contours are presented in Fig. 16. Again, these show that low momentum fluid from the trailing-edge shear-layer, colored in blue, become entrained into the leading-edge vortex within a very short distance from the trailing-edge. The vortex itself in general has velocity higher than that of freestream for the first four stations, but zones of localized lower velocity appear around the core with increasing distance downstream as described previously in the paper.

The evolution of the various properties in the core with respect to their trailing-edge values is presented in Fig. 17. The circulation was calculated by performing the line-integration of the crossflow velocity field. It can be seen that while the complicated process of mass entrainment is taking place in the near-wake, the circulation remained fairly constant. At the same time, it is observed that when significant entrainment of the shear-layer fluid into the core commenced, as indicated by turbulence intensity, the maximum velocity decreases rapidly. These trends are consistent with the qualitative prediction from Eq. (1) discussed earlier.

4. Concluding Remarks

A quantitative comparison of the leading-edge vortices in the near-wake for incompressible and supersonic flows has been made. The results indicate that quantitative similarities exist in the distributions of total pressure and swirl velocity. In both flow regimes, the planform produced primary and secondary vortices with similar topological features. The trajectory of the vortices was likewise found to be similar. However, at the trailing-edge the vortex core at the Mach 2.49 case was found to be significantly elongated in the spanwise direction. In comparison, the core in the low-speed counterpart was relatively round and actually somewhat elongated in the transverse direction at the higher angle-of-attack. With increasing distance downstream the core became more elongated in the transverse direction for all cases. This "switchover" of the cross-sectional shape was most pronounced at the higher angle-of-attack in the Mach 2.49 case. The results also showed that the secondary vortex disappeared completely, by half-chord downstream from the trailing-edge, in the low-speed case but not at the Mach 2.49 case. The most conspicuous difference was noted in the axial velocity trends. The details of the axial flow were shown to depend on complicated interaction of the circulation and viscous loss generated by the planform. It was shown that a jet-like profile either locally or globally, is increasingly unlikely as compressibility increases. It is therefore conceivable that vortices generated in a higher Mach number flow would be more prone to breakdown due to the velocity deficit. The extrapolation of low-speed vortex flow information beyond basic flow visualization is therefore not recommended, especially at high angles-of-attack. The detailed flow mapping at low-speed provided a database for validating predictive tools, and insights into the near-field evolution of the vortex-wake.

Acknowledgments

The first author held a National Research Council Associateship at NASA Glenn Research Center when the low-speed experiments were performed and the

manuscript was prepared. The work was supported by Aerospace Propulsion Power Research and Technology Base Program.

References

[1]Spreiter, J. R., and Sacks, A. H., "The Rolling Up of the Trailing Vortex Sheet and Its Effect on the Downwash Behind Wings," *Journal of the Aeronautical Sciences*, Vol. 18, No. 1, January 1951, pp. 21-32, 72.

[2]Hummel, D., "On the Vortex Formation Over a Slender Wing at Large Angles of Incidence," *High Angle of Attack Aerodynamics, AGARD-CP-247*, 1978, pp. 13.1-13.17.

[3]Hiremath, B. M., Holla, V. S., and Govindaraju, S. P., "Study of Flow Field in the Near Wake of Delta Wings," *The Journal of Aeronautical Society of India*, Vol. 36, No. 1, February 1984, pp. 17- 27.

[4]Kedzie, C. R., and Griffin, K. E., "Experimental Measurements of Wake Characteristics of Low Aspect-Ratio Delta and Flapped-Plate Planforms," *USAFA-TN-83-6*, March 15, 1983.

[5]Wood, R., Wilcox, Jr., F. J., Bauer, S. X. S., and Allen, J. M., "High Speed Vortex Flows," AIAA Paper 2000-2215, 2000.

[6]Milanovic, I. M., and Wang, F. Y., "Experimental Studies on Compressible Leading-Edge Vortices," ASME Paper FEDSM2001-18117, *Proceedings of the 2001 ASME Fluids Engineering Division Summer Meeting*, 2001.

[7]Stanbrook, A., and Squire, L. C., "Possible Types of Flow at Swept Leading Edges," *Aeronautical Quarterly*, Vol. 15, Pt. 1, 1964, pp. 72-82.

[8]Stromberg, A., Henze, A., Limberg, W., and Krause, E., "Investigation of Vortex Structures on Delta Wings," *Zeitschrift für Flugwissenschaften und Weltraumforschung*, Vol. 20, No. 2, 1996, pp. 71-79.

[9]Erickson, G. E., Peake, D. J., Del Frate, J., Skow, A. M., and Malcolm, G. N., "Water Facilities in Retrospect and Prospect – An Illuminating Tool for Vehicle Design," *Aerodynamic and Related Hydrodynamic Studies Using Water Facilities, AGARD-CP-413*, 1987, pp. 1.1-1.27.

[10]Kraft, E. M., "Vortex Flows," *Boundary Layer Simulation and Control in Wind Tunnels, AGARD-AR-224*, 1988, pp. 338-355.

[11]Örnberg, T., "A Note on the Flow Around Delta Wings," Kungl Tekniska Högskolan Institutionen För Flygteknik KTH Aero TN 38, Stockholm, 1954.

[12]Rom, J., High Angle of Attack Aerodynamics: Subsonic, Transonic, and Supersonic Flows, *Springer-Verlag*, New York, 1992, pp. 13-23.

[13]Monnerie, B., and Werlé, H., "Study of Supersonic and Hypersonic Flow About a Slender Wing at an Angle of Attack," *Hypersonic Boundary Layers and Flow Fields, AGARD-CP-30*, 1968, pp. 23.1-23.19.

[14]Green, S. I. (Ed.), Fluid Vortices, *Kluwer Academic Publishers*, Dordrecht, the Netherlands, 1995, pp. 297-303.

[15]Centolanzi, F. J., "Measured and Theoretical Flow Field Behind a Rectangular and a Triangular Wing up to High Angles of Attack at a Mach Number of 2.46," *NASA TN D-92*, 1959.

[16]Walker, H. J., and Stivers, Jr., L. S., "Investigation of the Downwash and Wake Behind a Triangular Wing of Aspect Ratio 4 at Subsonic and Supersonic Mach Numbers," *NACA RM A50I14a*, 1950.

[17]Wetzel, B. E., and Pfyl, F. A., "Measurements of Downwash and Sidewash Behind Cruciform Triangular Wings at Mach Number 1.4," *NACA RM A51B20*, 1951.

[18]Spahr, J. R., and Dickey, R.R., "Wind-Tunnel Investigation of the Vortex Wake and Downwash Field Behind Triangular Wings and Wing-Body Combinations at Supersonic Speeds," *NACA RM A53D10*, 1953.

[19]Ganzer, U., and Szodruch, J., "Vortex Formation Over Delta, Double-Delta and Wave Rider Configurations at Supersonic Speeds," *Aerodynamics of Hypersonic Lifting Vehicles, AGARD-CP-428*, 1987, pp. 25.1-25.32.

[20]Povinelli, L. A., Povinelli, F. P., and Hersch, M., "A Study of Helium Penetration and Spreading in a Mach 2 Airstream Using a Delta Wing Injector," *NASA TN D-5322*, 1969.

[21]Fellows, K. A., and Carter, E. C., "Results and Analysis of Pressure Measurements on Two Isolated Slender Wings and Slender Wing-Body Combinations at Supersonic Speeds, Vol. 1 Analysis," *ARA Report No. 12*, November 1969.

[22]Craven, A. H. and Alexander, A. J., "An Investigation of Vortex Breakdown at Mach 2," *CoA Note Aero-158*, Cranfield College of Aeronautics, Cranfield, United Kingdom, 1963.

[23]Wendt, J., "Compressibility Effects on Flows Around Simple Components," *High Angle-of-Attack Aerodynamics, AGARD-LS-121*, 1982, pp. 7.1-7.20.

[24]Stallings, Jr., R. L., "Low Aspect Ratio Wings at High Angles of Attack," Tactical Missile Aerodynamics: General Topics, *Progress in Astronautics and Aeronautics Volume 141* (Editor: Hemsch, M. J.), 1992, pp. 251-286.

[25]Vorropoulos, G., and Wendt, J., "Laser Velocimetry Study of Compressible Effects on the Flow Field of a Delta Wing," *Aerodynamics of Vortical Type Flows in Three Dimensions, AGARD-CP-342*, 1983, pp. 9.1-9.13.

[26]McGregor, I., "Development of the Vapor Screen Method of Flow Visualization in a 3 Ft. x 3 Ft. Supersonic Tunnel," *Flow Visualization in Wind Tunnels Using Indicators, AGARDograph 70*, 1962, pp. 115-164.

[27]Lee, M., and Ho, C.-M., "Vortex Dynamics of Delta Wings," Frontiers in Experimental Fluid Mechanics, *Springer-Verlag, Berlin*, 1989, pp. 365-427.

[28]Milanovic, I. M., and Kalkhoran, I. M., "Measurements of Leading Edge Vortices on a 75 Degree Delta Platform Wing at M = 2.5," AIAA Paper 2000-4002, 2000.

[29]Milanovic, I. M., and Kalkhoran, I. M., "Vortex-Wake Measurements of a Delta Wing in a Supersonic Stream," *Journal of Aircraft*, Vol. 38, No. 2, March – April 2001, pp. 315-325.

[30]Milanovic, I. M., and Kalkhoran, I. M., "Numerical Calibration of a Conical Five-Hole Probe for Supersonic Measurements," *Measurement Science and Technology*, November 2000, pp. 1812–1818.

[31]Foss, J. K., and Zaman, K. B. M. Q., "Large- and Small-Scale Vortical Motion in a Shear Layer Perturbed by Tabs," *Journal of Fluid Mechanics*, Vol. 382, 1999, pp. 307-329.

[32]Délery, J., Horowitz, E., Leuchter, O., and Solignac, J.-L, "Fundamental Studies on Vortex Flows," *La Recherche Aérospatiale (English Edition)*, No. 2, 1984, pp. 1-24.

[33]Nedungadi, A., and Lewis, M. J., "Computational Study of the Flow-Fields Associated with Oblique Shock/Vortex Interactions," *AIAA Journal*, Vol. 34, No. 12, 1996, pp. 2545–2553.

[34]Mahesh, K., "A Model for the Onset of breakdown in an Axisymmetric Compressible Vortex," *Physics of Fluids*, Vol. 8, No. 12, 1996, pp. 3338-3345.

[35]Kalkhoran, I. M., and Smart, M. K., "Aspects of Shock Wave-Induced Vortex Breakdown," *Progress in Aerospace Sciences*, Issue 36, No. 1, 2000, pp. 63-95.

[36]Batchelor, G. K., "Axial Flow in Trailing Line Vortices," *Journal of Fluid Mechanics*, Vol. 20, Part 4, 1964, pp. 645-658.

[37]Wang, F. Y., and Sforza, P. M., "Near-Field Experiments on Tip Vortices at Mach 3.1," *AIAA Journal*, Vol. 35, No. 4, April 1997, pp. 750-753.

[39]Werlé, H., "Le Tunnel Hydrodynamique au Service de la Recherche Aérospatiale," *ONERA TP-156*, 1974.

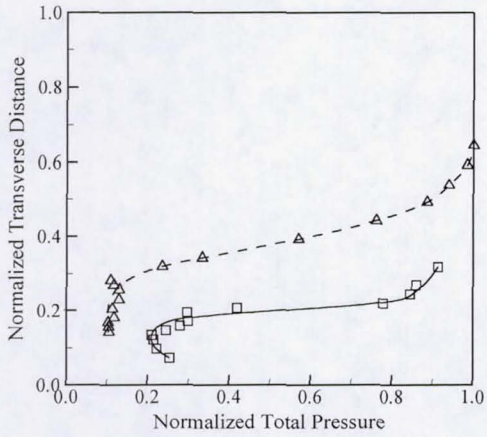

1a. Mach 2.49

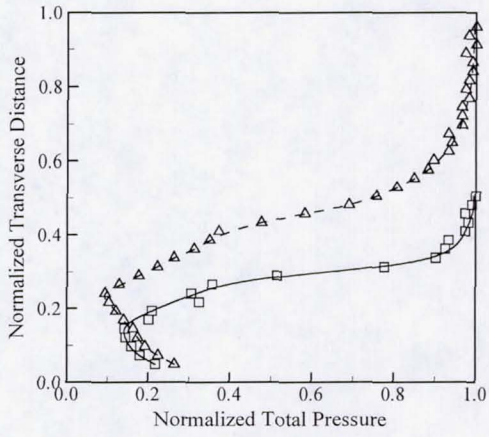

1b. Mach 0.02

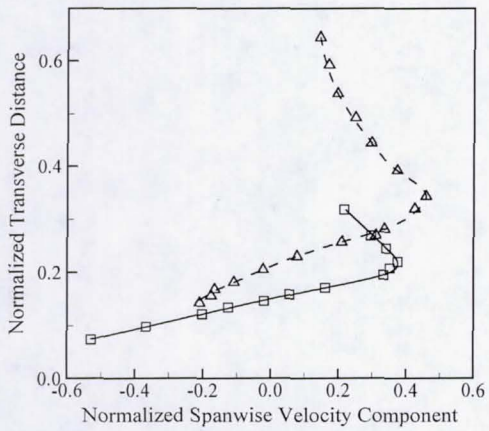

2a. Mach 2.49

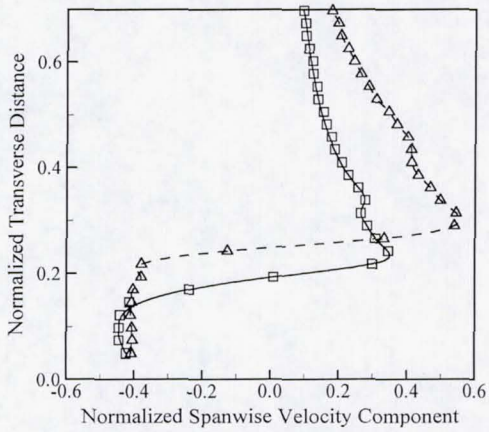

2b. Mach 0.02

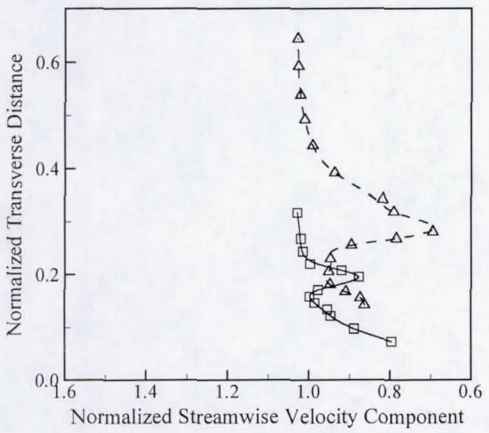

3a. Mach 2.49

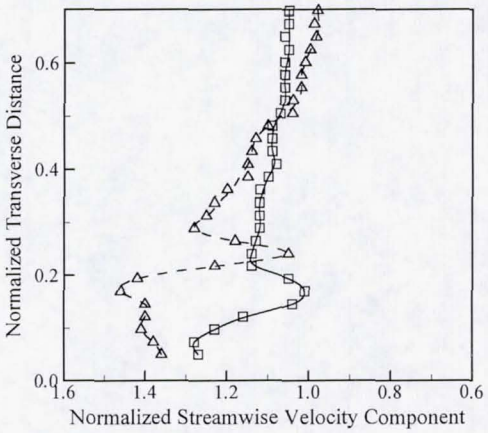

3b. Mach 0.02

Figs. 1-3 Comparison of Transverse Profiles at Trailing-Edge; □ $\alpha=7^{\circ}$, Δ $\alpha=12^{\circ}$.

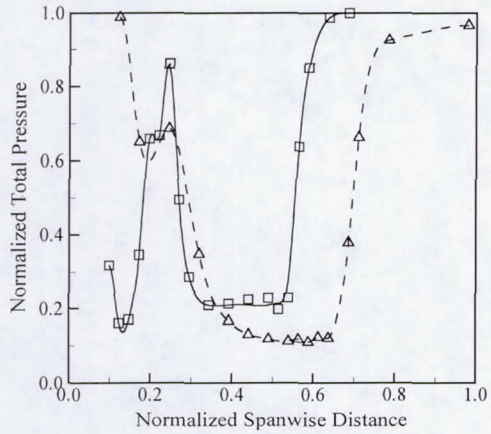

4a. Mach 2.49

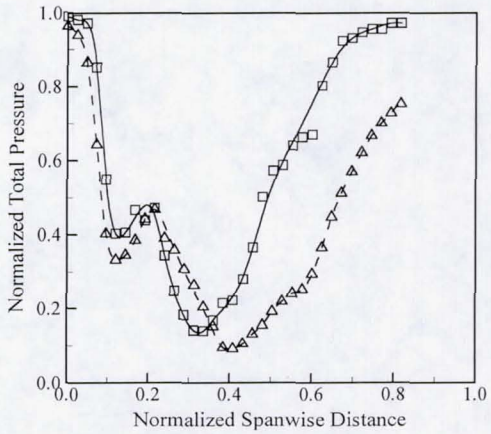

4b. Mach 0.02

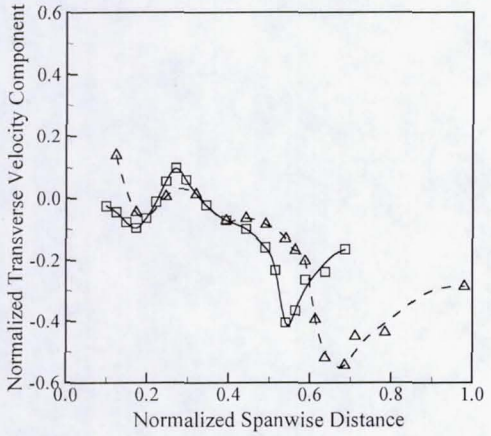

5a. Mach 2.49

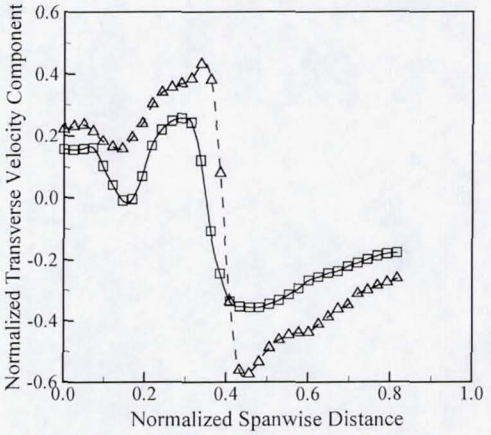

5b. Mach 0.02

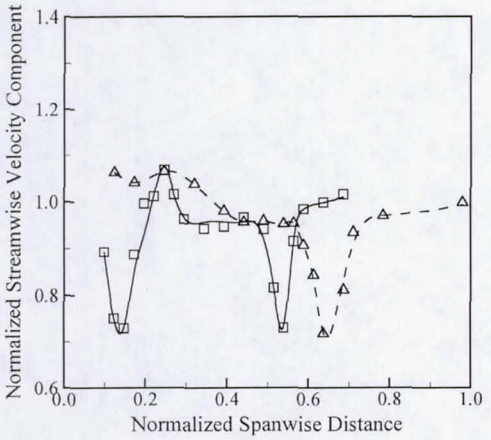

6a. Mach 2.49

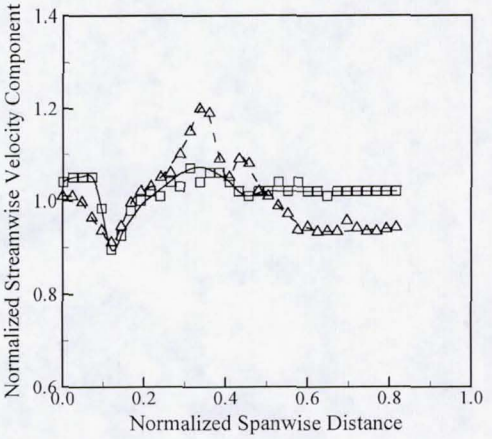

6b. Mach 0.02

Figs 4-6 Comparison of Spanwise Profiles at Trailing-Edge; □ $\alpha=7^\circ$, Δ $\alpha=12^\circ$.

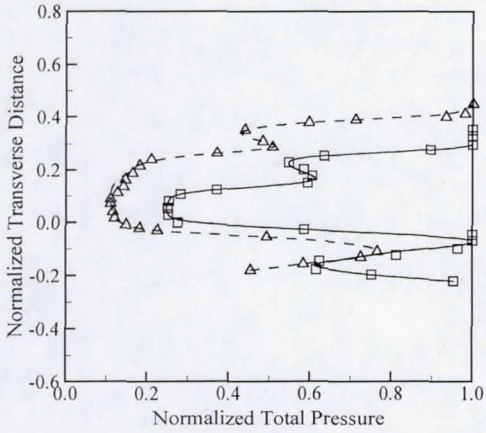

7a. Mach 2.49

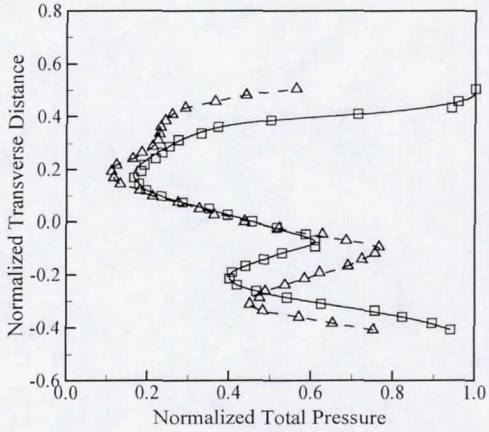

7b. Mach 0.02

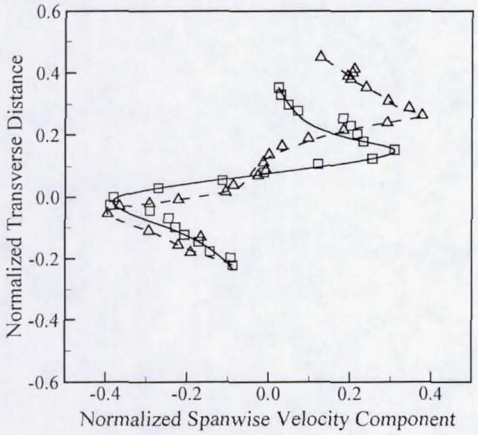

8a. Mach 2.49

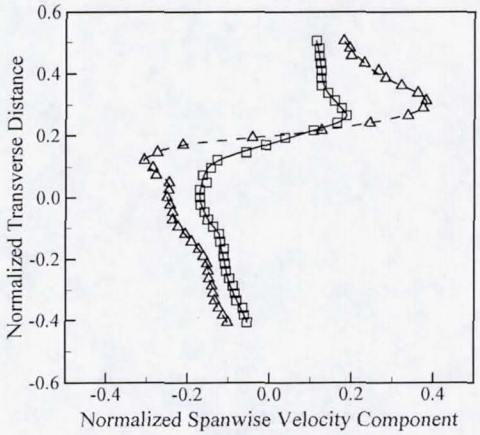

8b. Mach 0.02

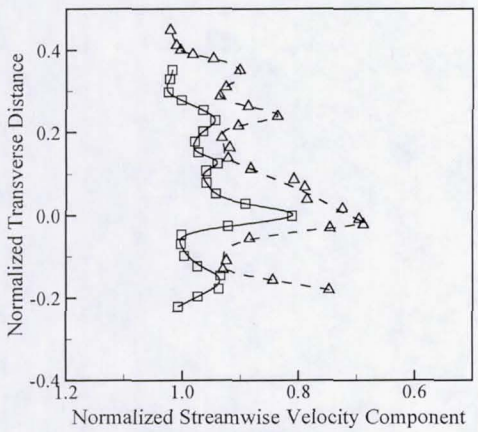

9a. Mach 2.49

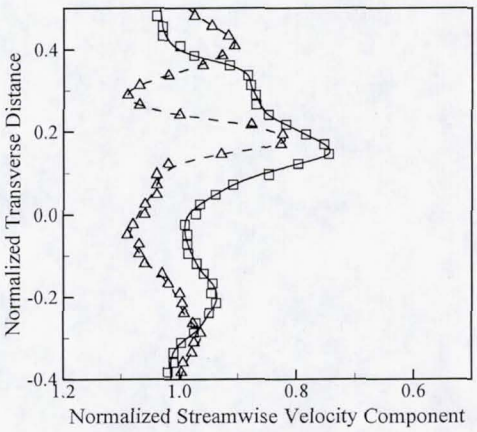

9b. Mach 0.02

Figs 7-9 Comparison of Transverse Profiles at Half-Chord Downstream; □ $\alpha=7^{\circ}$, Δ $\alpha=12^{\circ}$.

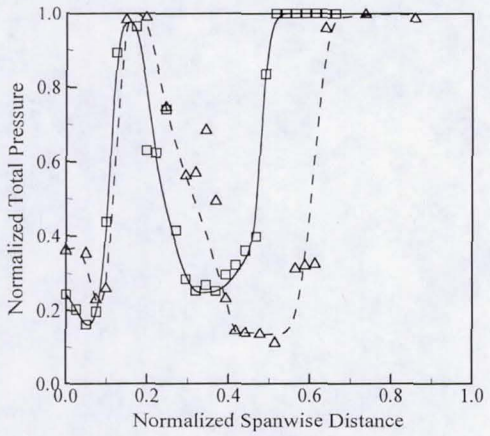

10a. Mach 2.49

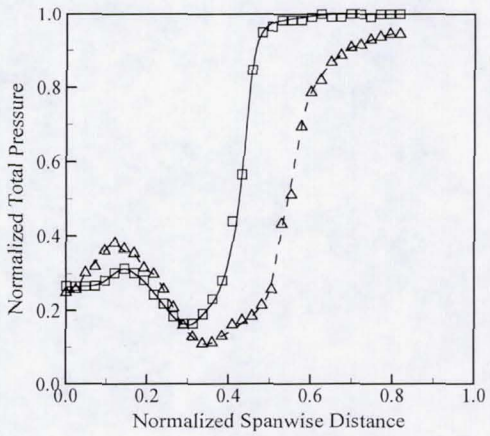

10b. Mach 0.02

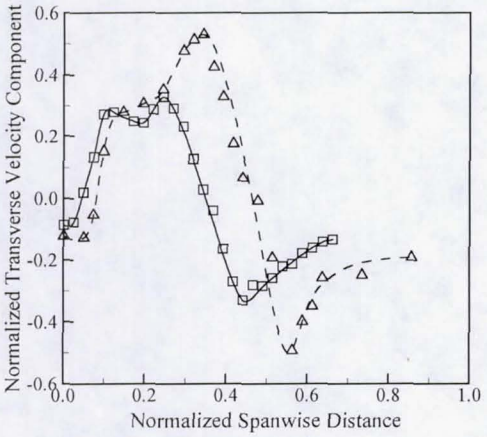

11a. Mach 2.49

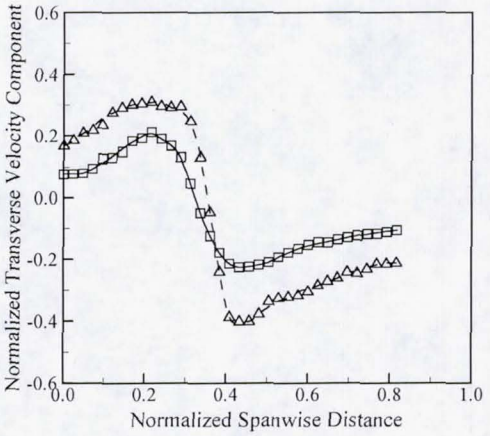

11b. Mach 0.02

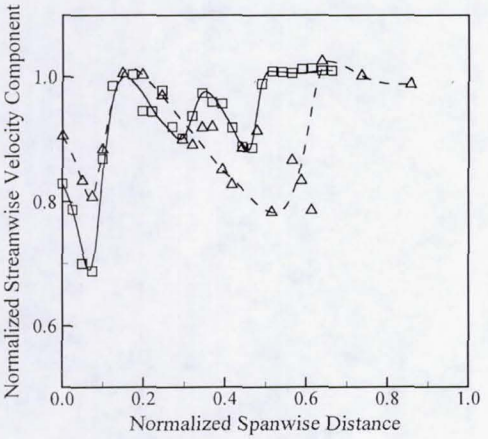

12a. Mach 2.49

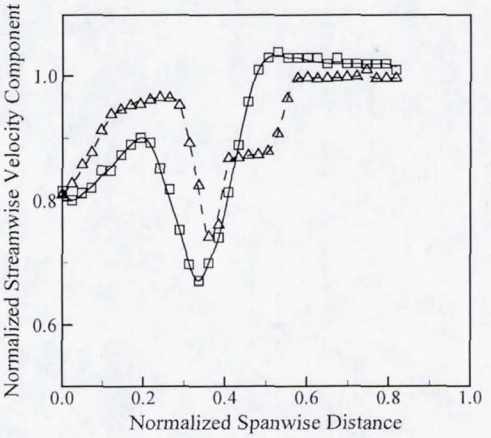

12b. Mach 0.02

Figs. 10-12 Comparison of Spanwise Profiles at Half-Chord Downstream; □ α=7° , Δ α=12°.

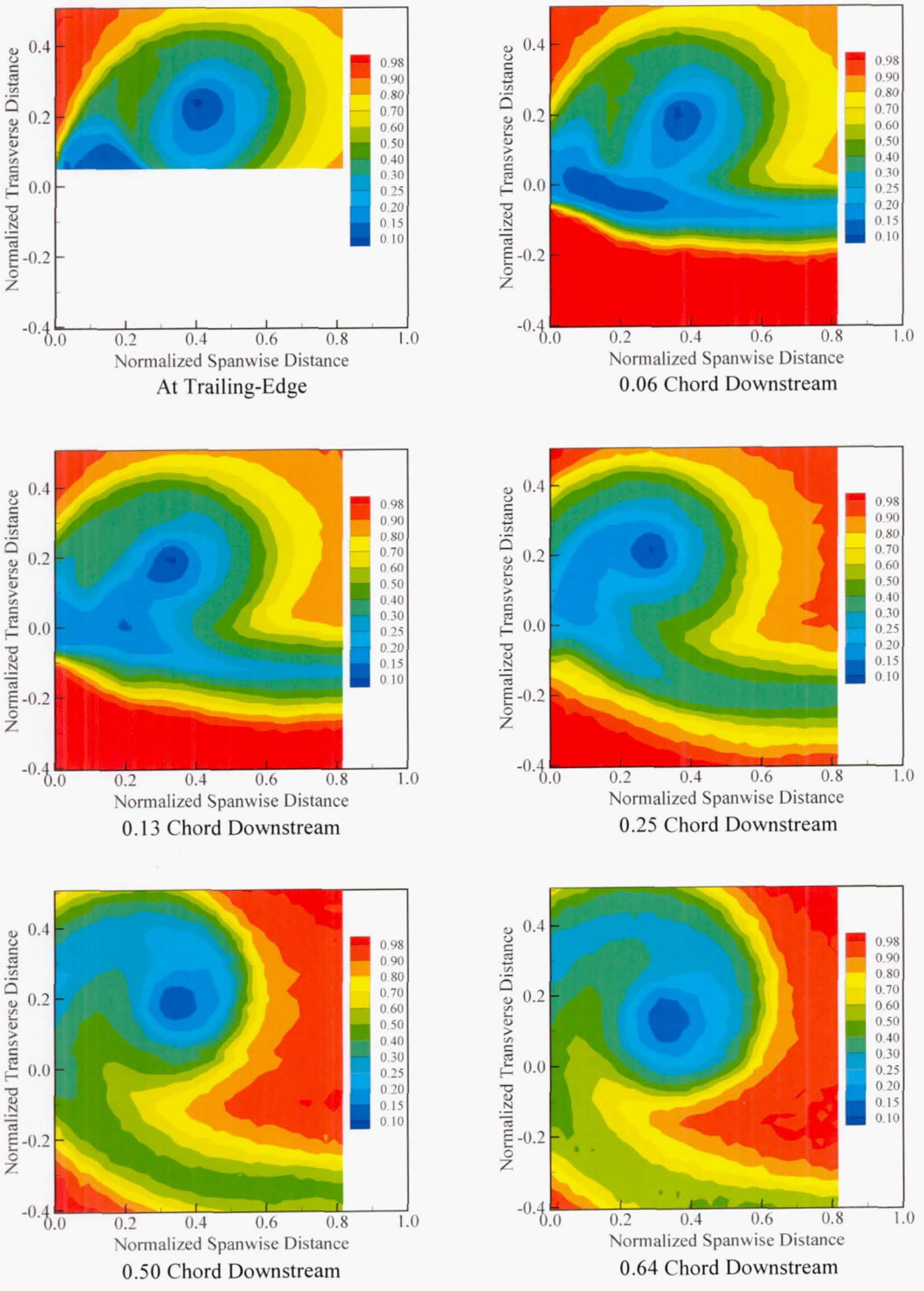

Fig. 13 Low-Speed Vortex-Wake Development at $\alpha=12^{o}$: Normalized Total Pressure.

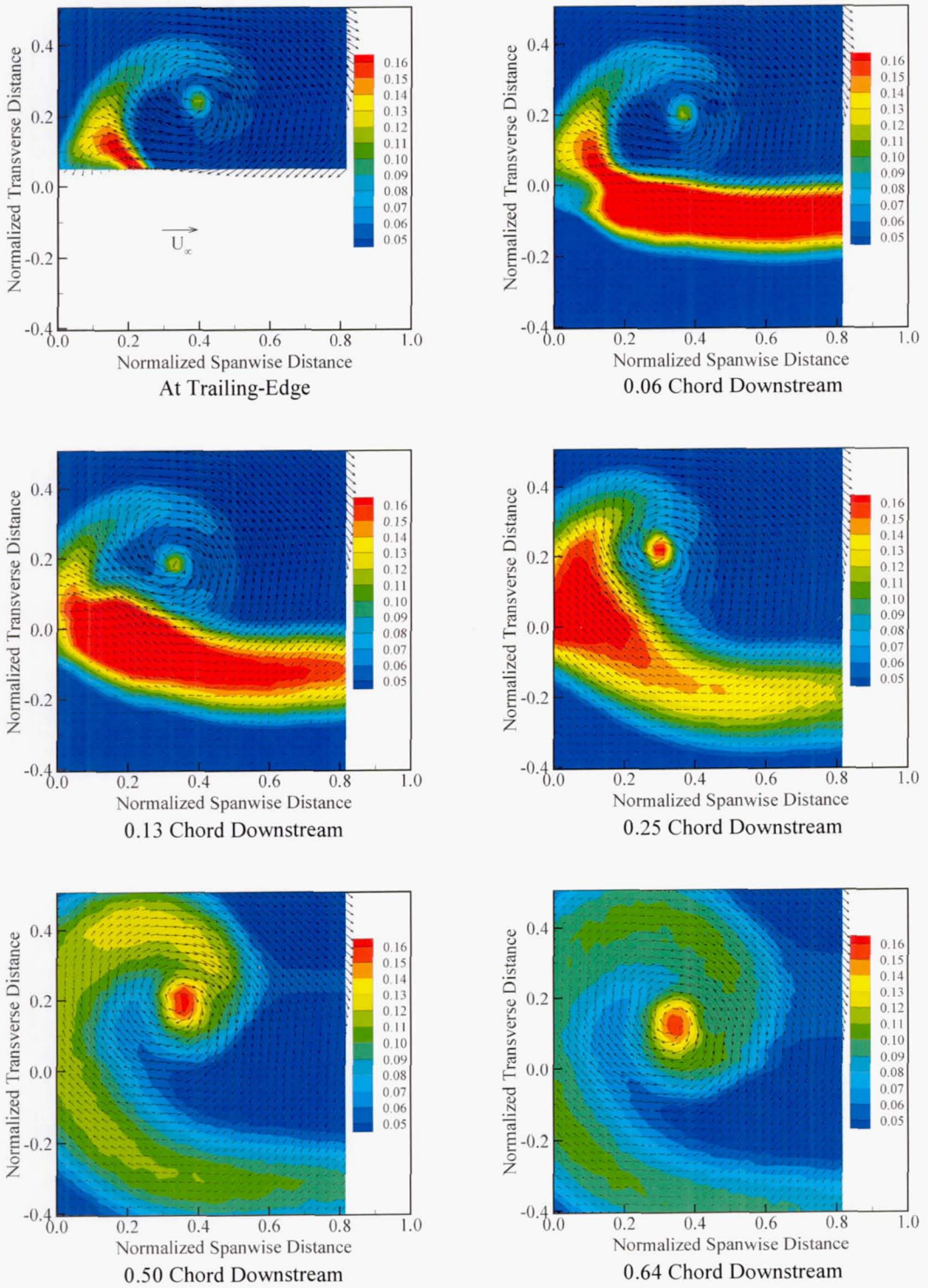

Fig. 14 Low-Speed Vortex-Wake Development at $\alpha=12^\circ$: Turbulence Intensity.

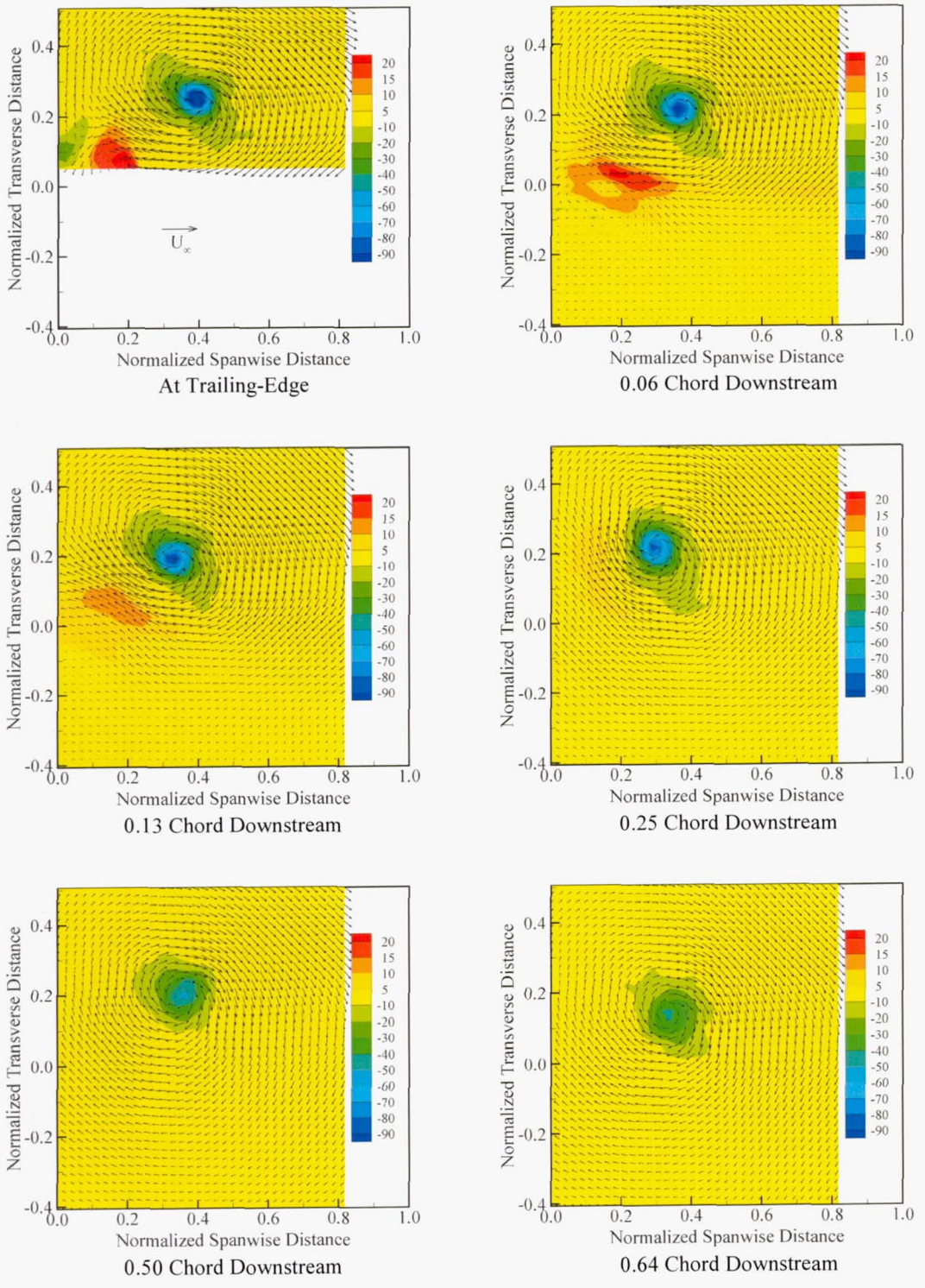

Fig. 15 Low-Speed Vortex-Wake Development at $\alpha=12^\circ$: Normalized Streamwise Vorticity.

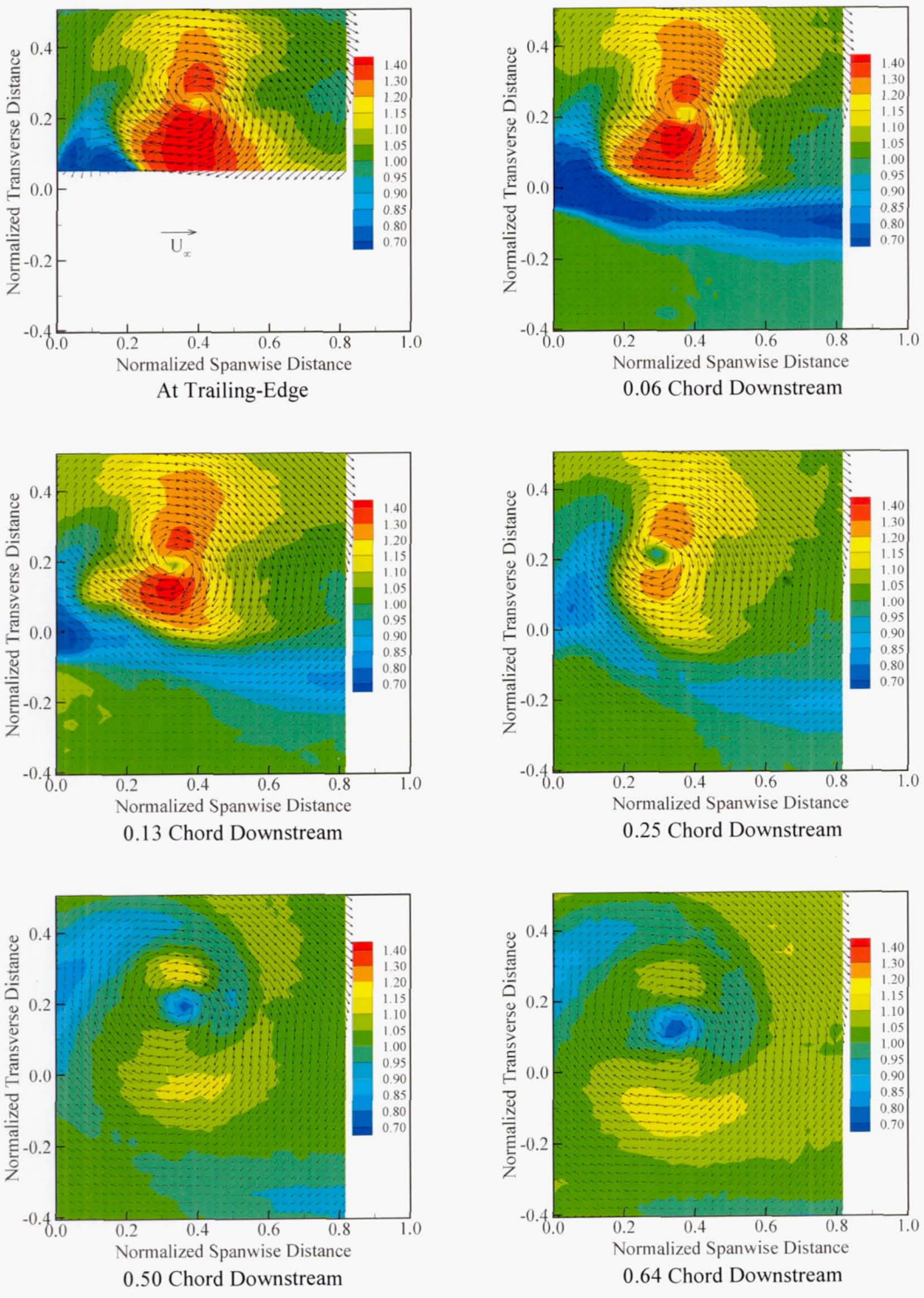

Fig. 16 Low-Speed Vortex-Wake Development at $\alpha=12^{\circ}$: Normalized Total Velocity.

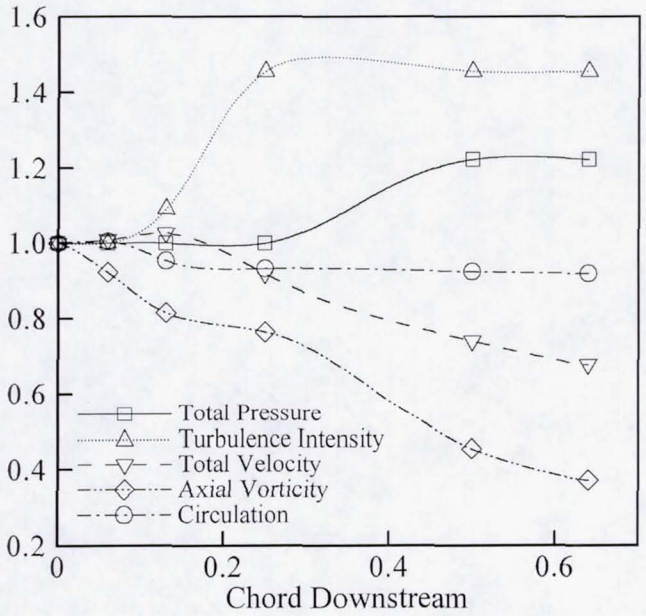

Fig. 17 Evolution of Minimum or Maximum Values of Various Properties Within the Vortex Core, Normalized by Respective Values at Trailing-Edge.